

LA-UR-

*Approved for public release;
distribution is unlimited.*

Title:

Author(s):

Submitted to:



Los Alamos National Laboratory, an affirmative action/equal opportunity employer, is operated by the University of California for the U.S. Department of Energy under contract W-7405-ENG-36. By acceptance of this article, the publisher recognizes that the U.S. Government retains a nonexclusive, royalty-free license to publish or reproduce the published form of this contribution, or to allow others to do so, for U.S. Government purposes. Los Alamos National Laboratory requests that the publisher identify this article as work performed under the auspices of the U.S. Department of Energy. Los Alamos National Laboratory strongly supports academic freedom and a researcher's right to publish; as an institution, however, the Laboratory does not endorse the viewpoint of a publication or guarantee its technical correctness.

Form 836 (8/00)

LANL Report LA-UR-98-5999 (1998)

Talk given at the *Fourth Workshop on Simulating Accelerator Radiation Environments (SARE4)*, Knoxville, Tennessee, September 14-16, 1998

Improved Cascade-Exciton Model of Nuclear Reactions

Stepan G. Mashnik and Arnold J. Sierk

T-2, Theoretical Division, Los Alamos National Laboratory, Los Alamos, NM 87545

Abstract

Recent improvements to the Cascade-Exciton Model (CEM) of nuclear reactions are briefly described. They concern mainly the cascade stage of reactions and a better description of nuclei during the preequilibrium and evaporation stages of reactions. The development of the CEM concerning fission is given in a separate talk at this conference. The increased accuracy and predictive power of the CEM are shown by several examples. Possible further improvements to the CEM and other models are discussed.

1. Introduction

During the last two decades, several versions of the Cascade-Exciton Model (CEM) [1] of nuclear reactions have been developed at JINR, Dubna. A large variety of experimental data on reactions induced by nucleons [2], pions [3], and photons [4] has been analyzed in the framework of the CEM and the general validity of this approach has been confirmed. Recently, the CEM has been extended by taking into account the competition between particle emission and fission at the compound nucleus stage and a more realistic calculation of nuclear level density [5]. In the last few years, the CEM code has been modified [6, 7] to calculate hadron-induced spallation and used to study [6]–[12] about 1000 reactions induced by nucleons from 10 MeV to 5 GeV on nuclei from Carbon to Uranium.

At present, several versions of the CEM code are used at a number of national laboratories and universities to solve different problems. Several versions of the CEM code have been implemented with or without modifications into a number of well-known transport codes, e.g., in: MARS [13], HETC [14, 15], TIERCE [16], MCNPX [17], and is currently being incorporated into the LLNL radiation-transport code COG [18]. The preequilibrium part of the CEM has been implemented either as the initial Modified Exciton Model (MEM) code MODEX [19] or as the later version from [20] wholly or with some modifications into the transport codes HETC96 [21, 15], SHIELD [22], HETC-3STEP [23, 15], HETC-FRG [24, 15], CASCADE [25], and into the intranuclear cascade-preequilibrium-evaporation-fission code INUCL [26].

The recent *International Code Comparison for Intermediate Energy Nuclear Data* [27] has shown that the CEM adequately describes nuclear reactions at intermediate energies and has one of the best predictive powers for double differential cross sections of secondary nucleons as compared to other available models (see Tabs. 5 and 6 in the Report [27] and Fig. 7 in Ref. [28]). As an example, in Fig. 1 we show experimental spectra of neutrons emitted from interactions of 1.5 GeV protons with C, Al, Fe, In, and Pb [29] compared with calculations using a version of the CEM as realized in the code CEM95 [20]. We see that CEM95 reproduces the data very well. In effect, these results can be regarded as a prediction of CEM95, as the experimental data were published in 1997 while the calculations are made without any changes of the code and using the previously determined “preferred” set of input parameters (RM=1.5, IFAM=9, IDEL=0, ISH=6, ISHA=1, IDELTA=1; see notations and details in the CEM95 code manual [20]); these were fixed in 1995.

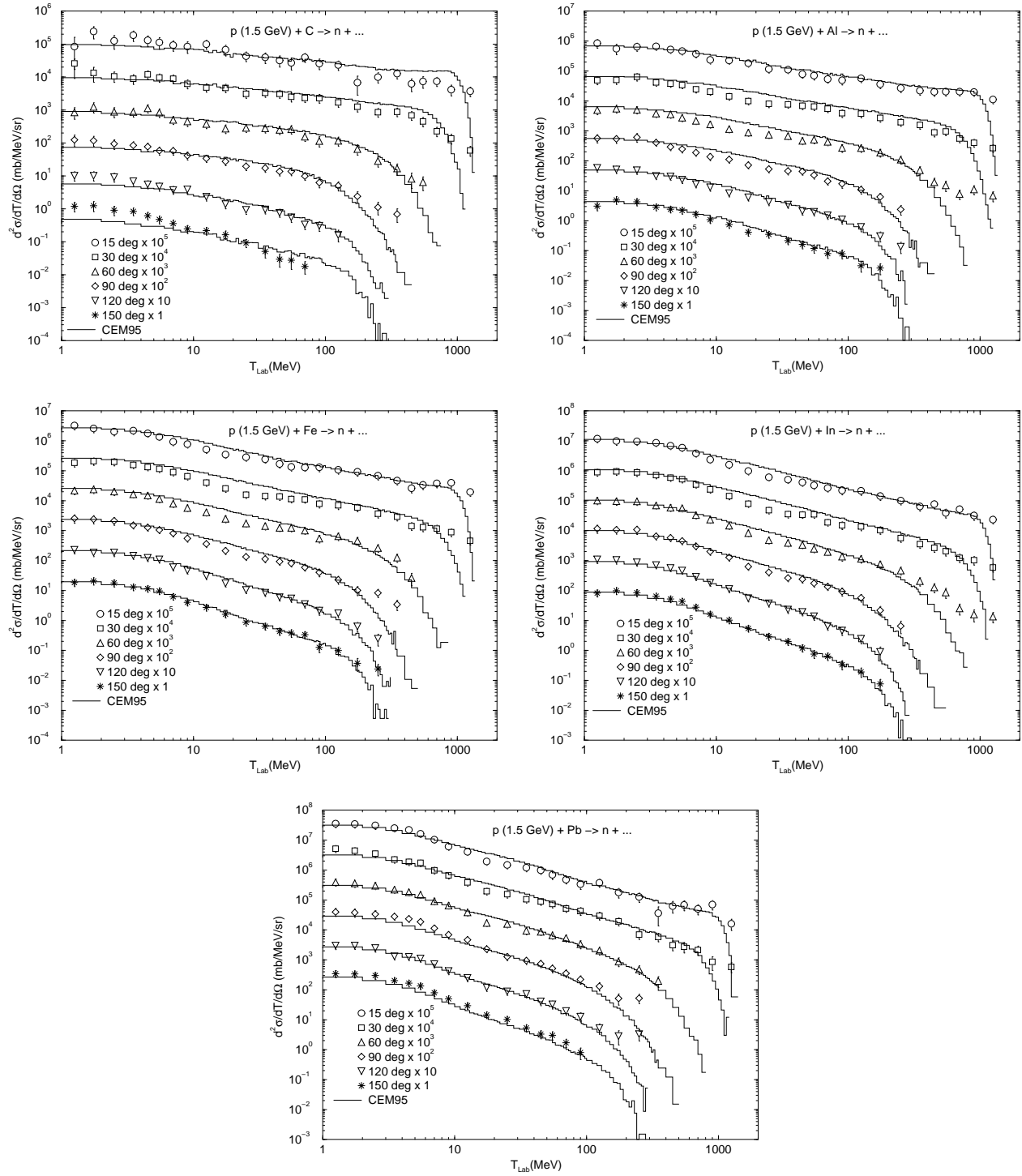


Fig. 1. Comparison of measured [29] double differential cross sections of neutrons from 1.5 GeV protons on C, Al, Fe, In, and Pb with CEM95 calculations.

Unfortunately, not all CEM95 results agree so remarkably well with measurements. As an example, Fig. 2 shows also experimental spectra of neutrons emitted from interactions of 256 MeV protons with Al [30], Fe [30], and Zr [31], and 1.5 GeV π^+ with Fe [32]. Calculations with CEM95 using the same

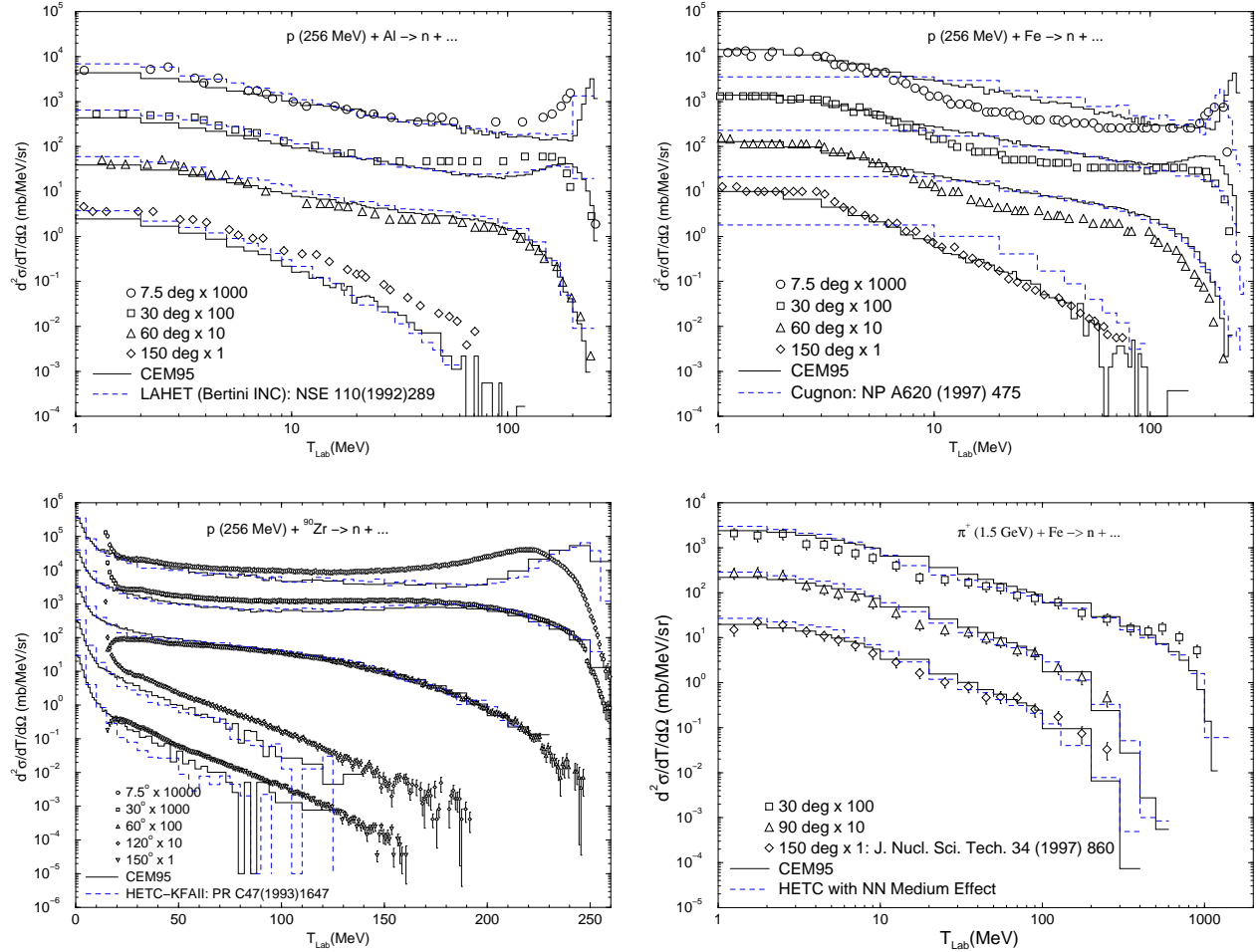


Fig. 2. Comparison of measured neutron spectra from 256 MeV protons on Al [30], Fe [30], and Zr [31], and 1.5 GeV π^+ on Fe [32] with CEM95 calculations (solid histograms) and with results of LAHET [33] for Al from [30], prediction of the recently improved version of the Cugnon et al. INC [34] for Fe, HETC-KFAII [35, 15] calculations for Zr from [31], and a Japanese version [36] of HETC [15] using modified NN cross sections to take account of the in-medium effects for $\pi^+(1.5 \text{ GeV})+\text{Fe}\rightarrow n+\dots$ from Ref. [32], shown by dashed histograms.

fixed set of input parameters as for Fig. 1 are shown by solid histograms. For comparison, results obtained with other well-known codes are shown as well: LAHET [33] calculations for Al from [30], a recent improved version of the Liège INC model by Cugnon et al. [34] for Fe, a Jülich version of HETC [15] as realized in the code HETC-KFAII [35] for Zr from [31], and a recent Japanese version [36] of HETC [15] using modified NN cross sections to take account of the in-medium effects for $\pi^+(1.5 \text{ GeV})+\text{Fe}\rightarrow n+\dots$ from Ref. [32].

One can see that for these reactions the agreement of CEM95 results with the measured neutron spectra is not as good as that shown in Fig. 1; in places the difference is bigger than a factor of 2. This seems to be a characteristic of all the models compared here.

For any model, to predict yields of isotopes produced at intermediate energies is much more difficult than to calculate spectra of emitted particles [37]. As one can see from Figs. 3 and 4 (adapted from [38]), CEM95 describes the majority of yields for isotopes produced in the spallation region quite well and no worse than other well-known codes, although for some individual isotopes the discrepancy with the

Products in Bi-209 irradiated with 0.13GeV protons

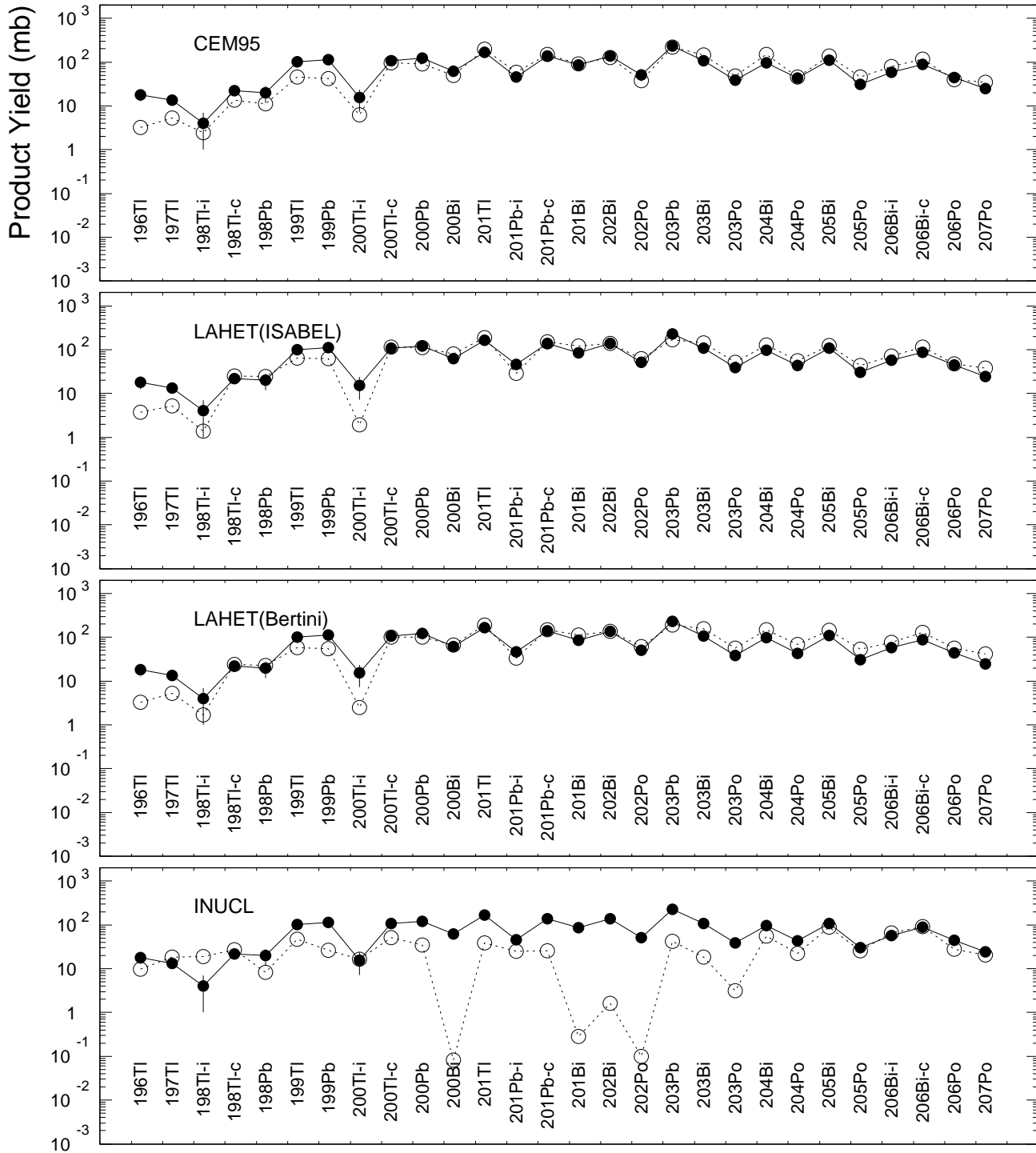


Fig. 3. Comparison between experimental data [38] (filled circles) and calculations with the codes CEM95 [20], LAHET [33], and INUCL [26] of yields of the indicated isotopes from ^{209}Bi irradiated with 130 MeV protons.

Products in Bi-209 irradiated with 0.13GeV protons

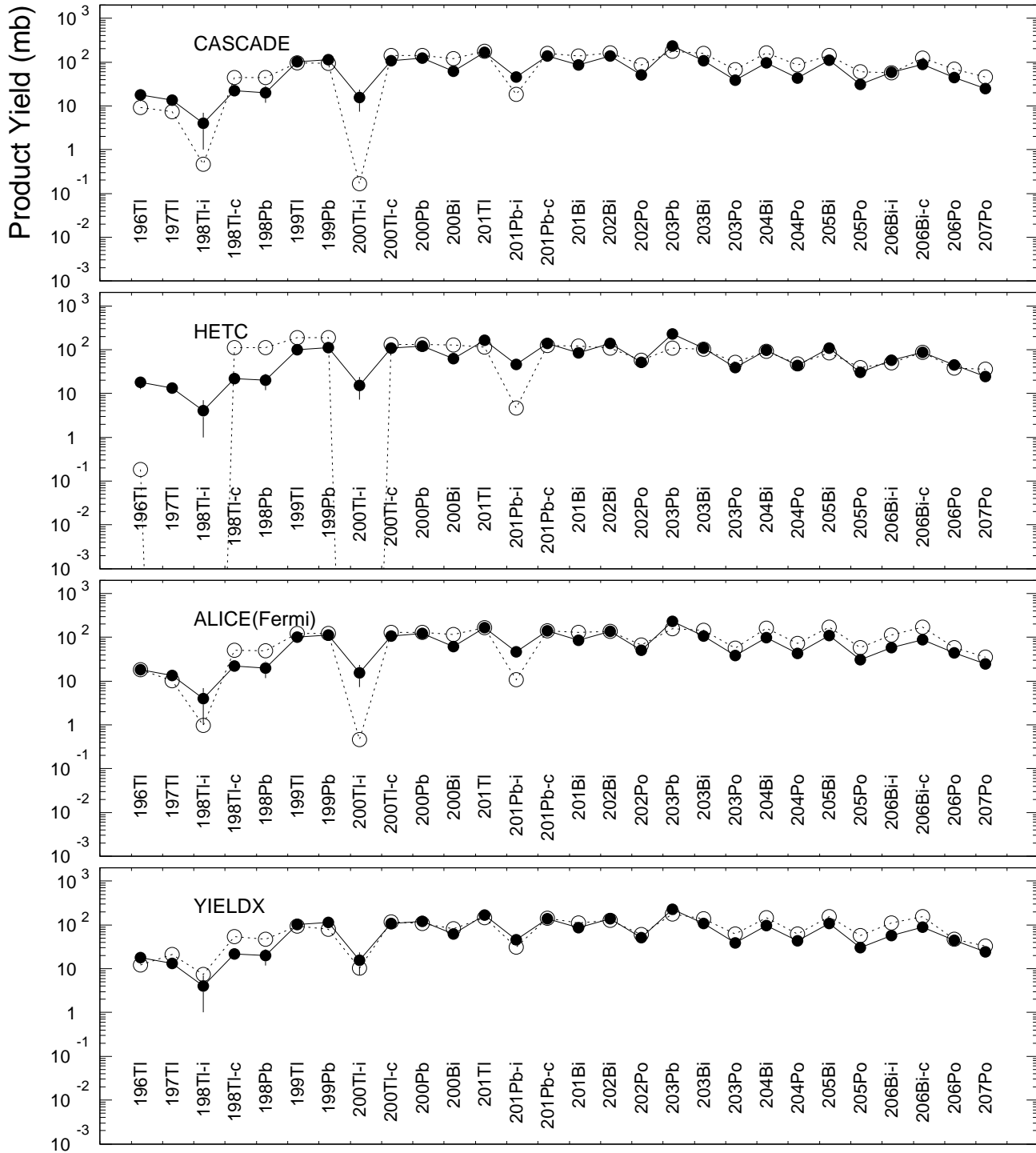


Fig. 4. The same as Fig. 3 using instead calculations with the CASCADE [25], HETC [15], HMS-ALICE [39] codes, and YIELDX phenomenological systematics [40].

cross sections. measurements is quite large.

The recent projects for Accelerator Transmutation of Waste (ATW) and Accelerator Production of Tritium (APT) have revived interest in accurate nuclear reaction data at intermediate energies (see, e.g., [41]). Not all needed data can be measured, therefore reliable models are required to provide the necessary. This is our motivation for attempting to improve the CEM into a model capable of predicting reliable nuclear cross sections for arbitrary targets in a wide range of incident energies.

The philosophy of our work is not just to include a few more parameters, fitting them to describe the available data, a commonly used practice in development of codes for applications. Instead, we are further developing the CEM by progressively incorporating features of previously neglected physics, striving meanwhile not to destroy the current broad strengths of CEM95 and its good predictive power. To investigate the dependence of theoretical results on the physics incorporated in CEM95 and to identify the improvements to the CEM and to other similar models which are of highest priority, we have performed a detailed analysis of more than 600 excitation functions for proton-induced reactions on 19 targets from C to Au at energies from 10 MeV to 5 GeV [7]. After this analysis, we created a list of potential improvements to the CEM95 code [7]. Some these have already been incorporated and we describe them briefly in the present paper. Nevertheless, as we have not yet completed our work, some of the results presented below are still preliminarily.

2. The Main Concepts of the Model

A detailed description of the CEM may be found in Ref. [1] and of its extended version, as realized in the code CEM95, in Refs. [6, 7]; therefore, we mention here only its basic assumptions and features modified in the present work, for the sake of clarity. The CEM assumes that reactions occur in three stages. The first stage is the intranuclear cascade in which primary and secondary particles can be rescattered several times prior to absorption by, or escape from the nucleus. The cascade stage of the interaction is described by the standard version of the Dubna intranuclear cascade model (INC) [42]. The excited residual nucleus remaining after the emission of the cascade particles determines the particle-hole configuration that is the starting point for the second, preequilibrium stage of the reaction. The subsequent relaxation of the nuclear excitation is treated by an extension of the Modified Exciton model (MEM) [19] of preequilibrium decay which also includes a description of the equilibrium evaporative third stage of the reaction.

All the cascade calculations are carried out in a three-dimensional geometry. The nuclear matter density $\rho(r)$ is described by a Fermi distribution with two parameters taken from the analysis of electron-nucleus scattering, namely

$$\rho(r) = \rho_p(r) + \rho_n(r) = \rho_0 \{1 + \exp[(r - c)/a]\}, \quad (1)$$

where $c = 1.07A^{1/3}$ fm, A is the mass number of the target, and $a = 0.545$ fm. For simplicity, the target nucleus is divided by concentric spheres into seven zones in which the nuclear density is considered to be constant. The energy spectrum of the target nucleons is estimated in the perfect Fermi gas approximation with the local Fermi energy $T_F(r) = \hbar^2[3\pi^2\rho(r)]^{2/3}/(2m_N)$, where m_N is the nucleon mass. The influence of intranuclear nucleons on the incoming projectile is taken into account by adding to its laboratory kinetic energy an effective real potential V , as well as by considering the Pauli principle which forbids a number of intranuclear collisions and effectively increases the mean free path of cascade particles inside the target. For incident nucleons $V \equiv V_N(r) = T_F(r) + \epsilon$, where $T_F(r)$ is the corresponding Fermi energy and ϵ is the mean binding energy of the nucleons ($\epsilon \simeq 7$ MeV [42]). For pions, in the Dubna INC one usually uses [42] a square-well nuclear potential with the depth $V_\pi \simeq 25$ MeV, independently of the nucleus

and pion energy. The interaction of the incident particle with the nucleus is approximated as a series of successive quasifree collisions of the fast cascade particles (N or π) with intranuclear nucleons:

$$\begin{aligned} NN &\rightarrow NN, & NN &\rightarrow \pi NN, & NN &\rightarrow \pi_1, \dots, \pi_i NN, \\ \pi N &\rightarrow \pi N, & \pi N &\rightarrow \pi_1, \dots, \pi_i N & (i \geq 2). \end{aligned} \quad (2)$$

To describe these elementary collisions, we use experimental cross sections for the free NN and πN interactions, simulating angular and momentum distributions of secondary particles by special polynomial expressions with energy-dependent coefficients, and take into account the Pauli principle.

Besides the elementary processes (2), the Dubna INC also takes into account pion absorption on nucleon pairs

$$\pi + [NN] \rightarrow NN. \quad (3)$$

The momenta of two nucleons participating in the absorption are chosen randomly from the Fermi distribution, and the pion energy is distributed equally between these nucleons in the center-of-mass system of the pion and nucleons participating in the absorption. The direction of motion of the resultant nucleons in this system is taken as isotropically distributed in space. The effective cross section for absorption (let us speak below, for concreteness, e.g., about π^-) is estimated from the experimental cross-section for pion absorption by deuterons

$$\sigma(\pi^- + \text{“}np\text{”} \rightarrow nn) = W \cdot \sigma(\pi^- + d \rightarrow nn). \quad (4)$$

The quantity W can depend on the pion energy T_π , on the characteristics of the target nucleus, the point where the pion is absorbed, and on the spin-isospin states of absorbing pairs (see details and references in [3]).

3. Study Results

A. Elementary Cross-Sections. In the Dubna INC model [42] used in CEM95, the cross sections for the free NN and πN interactions (2) are approximated using a special algorithm of interpolation/extrapolation through a number of picked points, mapping as well as possible the experimental data. This was done very accurately by the group of Prof. Barashenkov using all experimental data available at that time, about 30 years ago. Currently, the experimental data on cross section is much richer, therefore we decided to revise the approximations of all elementary cross sections used in CEM95. We started with collecting all published experimental data from all available sources. Then, we developed an improved, as compared with the standard Dubna INC [42], algorithm for approximation of cross sections and developed simple and fast approximations for elementary cross sections which fit very well presently available experimental data not only to 5 GeV, the upper recommended energy for the present version of the CEM, but up to 50–100 GeV and higher, depending on availability of data. So far, we have such approximations for 34 different types of elementary cross sections induced by nucleons, pions, and gammas. Cross sections for other types of interactions taken into account in the CEM are calculated from isospin considerations using the former as input.

We consider this part of our CEM improvement as an independently useful development, as our approximations are reliable, fast, and easy to incorporate into any transport, INC, BUU, or Glauber-type model codes. For example, our new approximations recently have been successfully incorporated by N. Mokhov into the recent improved version of the MARS code system at Fermilab [13].

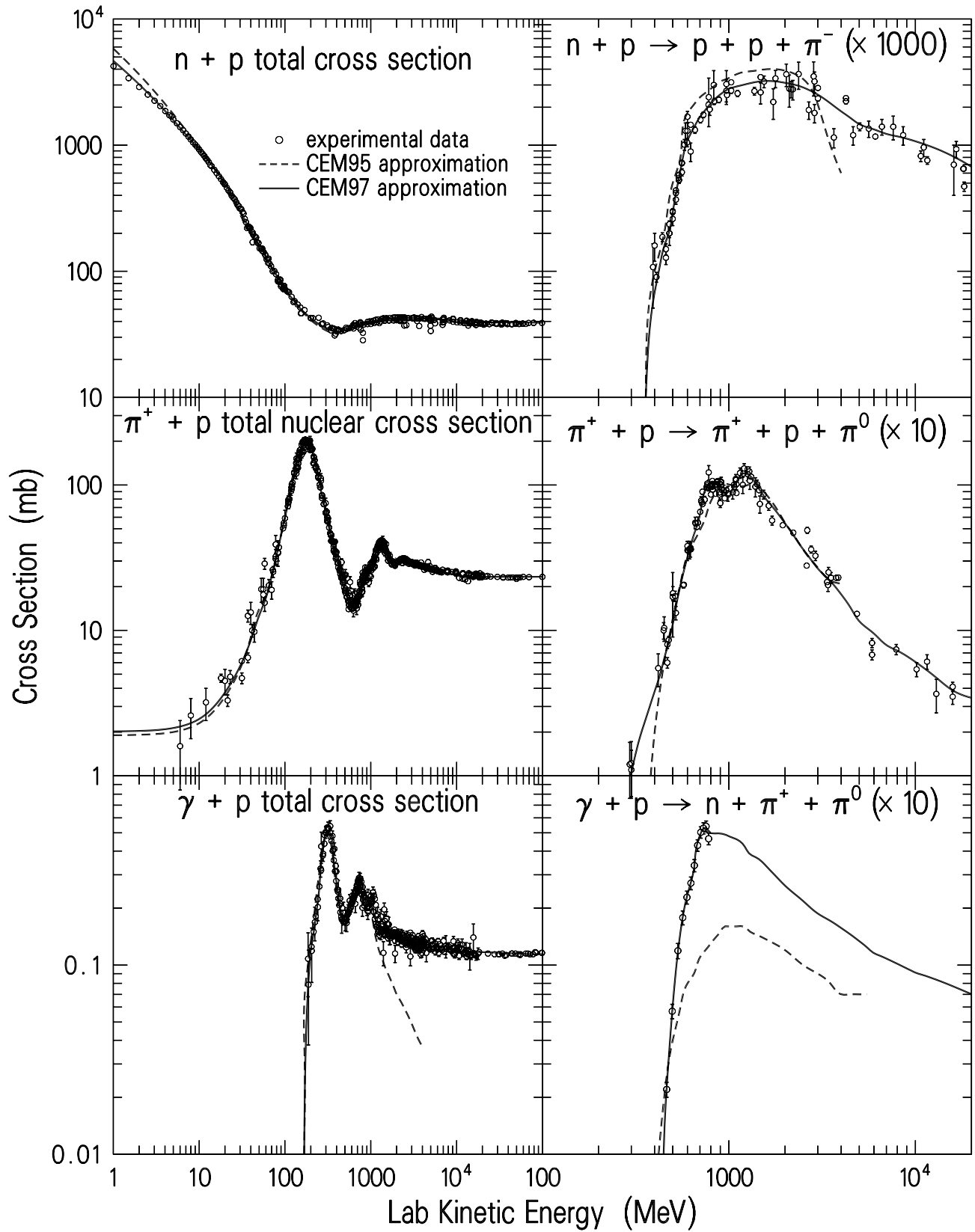


Fig. 5. Energy dependence of the np , π^+p , and γp total cross sections and of the $np \rightarrow pp\pi^-$, $\pi^+p \rightarrow \pi^+p\pi^0$, and $\gamma p \rightarrow n\pi^+\pi^0$ ones. Experimental points are from our compilation [43]. Solid lines are results of our present approximations; dashed lines show the standard Dubna INC approximations [42] used in CEM95.

We are going to publish our compilation of experimental data and our approximations of these cross sections in a separate paper and to make them available to users through the Web [43], as well as to make available to users our code for these approximations. An example of 6 compiled experimental cross sections together with our new approximations and the old approximations from CEM95 is shown in Fig. 5. We see that our new approximations describe indeed very well all data. Although presently we have much more data than 30 years ago when Barashenkov’s group produced their approximations used in CEM95, for a number of interaction modes like the total cross sections shown in the left panel of Fig. 5, the original approximations also agree very well with presently available data, in the energy region where the Dubna INC was developed to work. This is a partial explanation of why the old Dubna INC [42] and the younger CEM95 [20] work so well for the majority of characteristics of nuclear reactions.

On the other hand, for some modes of elementary interactions like the ones shown in the right panel of Fig. 5, the old approximations differ significantly from the present data, demonstrating the need for our present improvements for a better description of all modes of nuclear reactions.

B. Effects of Refraction and Reflection. In CEM95, the kinetic energy of cascade particles is increased or decreased as they move from one potential region (zone) to another, but their directions remain unchanged. That is, in our calculations, refraction or reflection of cascade particles at potential boundaries is neglected.

To understand how our results depend on effects of refractions and reflections we performed calculations for a number of reactions with a modified version of CEM95 taking into account refractions and reflections as described in the monograph [42] and realized by A. S. Iljinov [44]. An example of our results is shown on Fig. 6. From these and other similar results obtained for other reactions we conclude that refractions and reflections affect only weakly the spectra of secondary particles and somewhere more the total inelastic/elastic cross sections. As one could expect in advance, at low incident energies, refractions and reflections more strongly affect the calculated spectra but on the whole, CEM95 results without taking into account refractions and reflections agree better with the data, for the majority of analyzed reactions. Therefore, we prefer for our new version of the CEM to ignore refractions and reflections, as in the standard Dubna INC. We note that similar results were obtained earlier by Chen et al. [47].

C. Pion-Nucleus Potential V_π . It is natural that theoretical characteristics of a nuclear reaction involving pions depend on the pion-nucleus potential used in calculations. This problem has a history of almost half a century; it is not solved completely even now, and its review is beyond the scope of the present paper.

As mentioned above, CEM95 uses a constant attractive pion-nucleus potential of 25 MeV. This value was obtained 30 years ago by Barashenkov, Gudima, and Toneev [48] from an analysis of available data and was suggested as a basis for the Dubna INC. At the same time, analyzing pion-nucleus reactions at energies below 300 MeV and nuclear absorption of stopped antiprotons with the Dubna INC, Iljinov, Nazaruk, and Chigrinov suggested [49] that one can achieve a better agreement with the data using $V_\pi = 0$. Making the situation more confusing, in a recent extension of the Dubna INC for photonuclear reactions at energies up to 10 GeV by Iljinov et al. [50], a better description of pion photoproduction was achieved for $V_\pi = 35$ MeV.

Since previous INC studies of the values of V_π are based on analysis of quite scanty and old data, we decided to return once more to this question using the recent measurements at LAMPF of non-charge exchange (NCX) [51], single charge exchange (SCX) [45, 52], and double charge exchange (DCX) [53] pion production on targets from C to Bi in the energy region from 120 to 500 MeV.

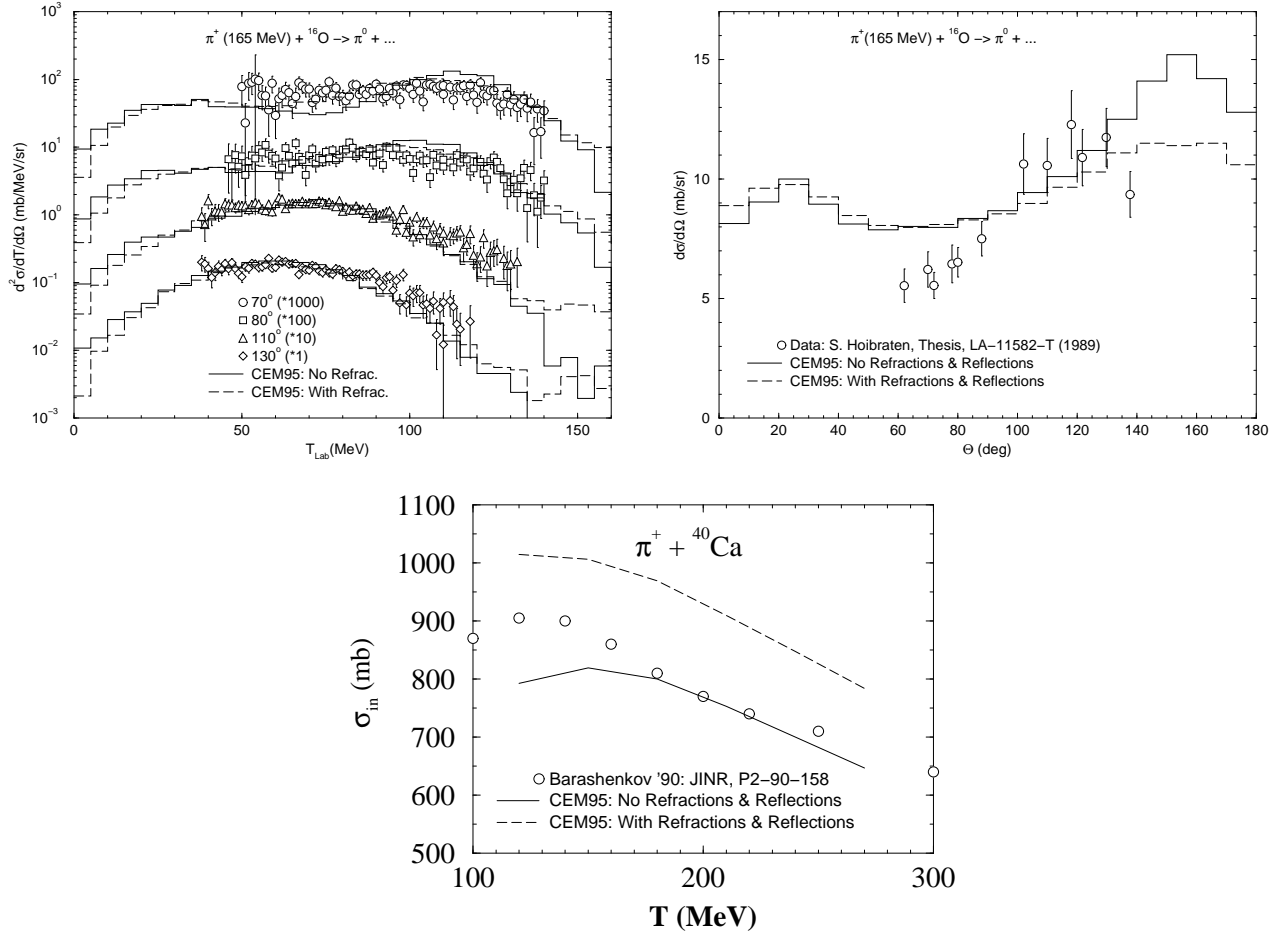


Fig. 6. Measured double differential spectra and angular distribution of π^0 from $\pi^+(165 \text{ MeV})+{}^{16}\text{O}$ [45] and Barashenkov's systematics [46] for the experimental $\pi^++\text{Ca}$ total inelastic cross section compared with CEM95 calculations without (solid) and with refractions and reflections (dashed).

We perform calculations for a large number of NCX, SCX, and DCX reactions using several values for V_π . An example of our results is shown in Fig. 7. Our analysis shows that total inelastic cross sections and mean multiplicities of secondary pions, as well as NCX and SCX pion spectra at incident energies well above the $\Delta(1232)$ resonance region depend only slightly on the value of V_π . But at lower incident energies corresponding to the $\Delta(1232)$ region the shapes of all NCX, SCX, and DCX spectra change significantly with changes in the value of V_π . Unfortunately, none of the fixed values of the V_π we try can provide a good simultaneous description of all data. Nevertheless, the best overall agreement with the different data we analyse is achieved using the original value of $V_\pi = 25 \text{ MeV}$.

Other recent studies show that V_π is a complex function of pion energy T_π , nuclear target (A, Z), radius vector r , and on the isospin of the pion. Ideally, for any INC model it would be useful to have a simple approximation for $V_\pi(A, Z, T_\pi, r)$ that could be used in simulations. We do not know any simple systematics for V_π , and it remains still an input parameter. For the moment, we choose $V_\pi = 25 \text{ MeV}$, with the understanding that this is not a final solution to the problem.

D. Pion Transparency. Transparency means an inhibition of the interaction of a pion with subsequent nucleons in the target nucleus for a certain time after creation of the pion. Recently, attention was called

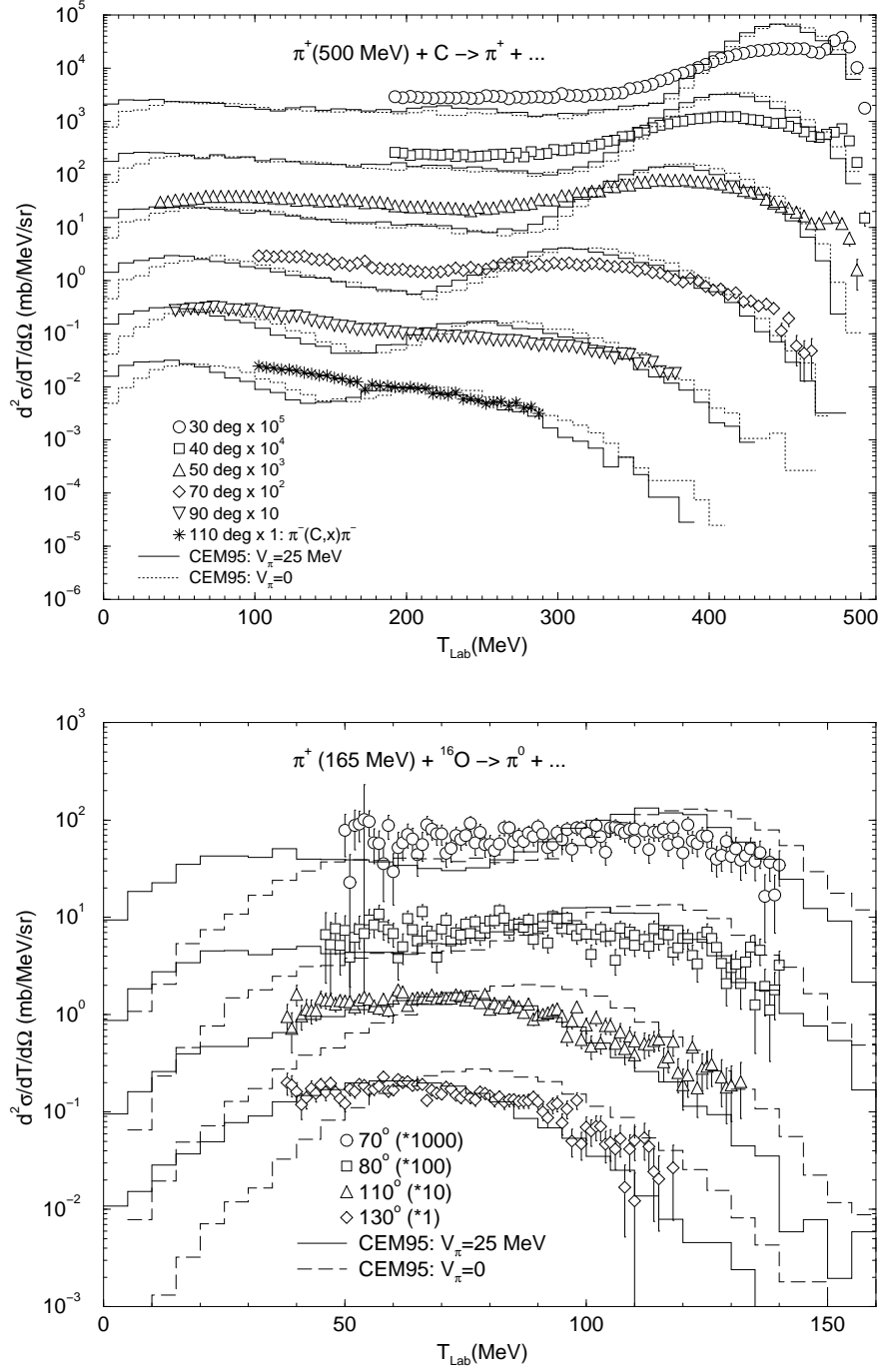


Fig. 7. Comparison of experimental NCX [51] and SCX [45] pion spectra for interactions of 500 MeV π^+ with C and 165 MeV π^+ with O with standard CEM95 results ($V_\pi = 25 \text{ MeV}$; solid histograms) and with calculations using $V_\pi = 0 \text{ MeV}$ (dashed histograms).

to this possible new physical effect after a study of the previously mentioned NCX pion production measurements at LAMPF [51] with the INC model by Gibbs et al. (GINC) [54]. GINC failed to reproduce the data, strongly underpredicting the measured yields at pion energies near 200 MeV. When pions in-

volved in $(\pi, 2\pi)$ reactions were not allowed to interact with the nucleus for a time equal to 2 fm/c, a considerable improvement in the agreement with data was achieved [51]. This fact was interpreted as a new phenomenon of nuclear pion transparency with several possible exotic sources like: a need for a hadronization time for the wave function of pions involved in pion production to settle into an eigenstate, a mechanism which allows the pions to be transported through the nucleus by weakly interacting σ mesons, or renormalized particle masses at central nuclear density [51]. Recently, we analyzed [55] SCX π^0 spectra from interactions of negative pions with ^{12}C and ^7Li at 467 and 500 MeV using the same GINC [54] and we got results very similar to the ones on NCX spectra published by Zumbro et al. [51]; we saw also an indication of some pion transparency.

Therefore we decided to implement this new piece of physics in the CEM, if appropriate. The Dubna INC used in CEM95 does not take into account the time of intranuclear elementary interactions, instead, it considers the coordinates of these interactions. So, instead of a hadronization time, we can require that the mean free path of secondary pions produced in $(\pi, 2\pi)$ reactions to be longer than a fixed value, e.g., 2 fm. Including a transparency distance of 2 fm for pions from $(\pi, 2\pi)$ interactions into the CEM improves the description of some of the NCX, SCX, and DCX pion spectra at pion incident energies around the $\Delta(1232)$ resonance region. An even better agreement with some of the data [51]–[53] is achieved by imposing a transparency of 2 fm for pions created in a $(\pi, 2\pi)$ interaction and, in addition, a transparency of 1.2 fm for all other pions involved in a reaction.

As we mentioned in the beginning, the aim of our work is to incorporate progressively in CEM95 new physical ingredients without destroying its present wholeness and good predictive power. Therefore we consider it necessary to analyze not only pion-induced NCX, SCX, and DCX reactions, but also other types of intermediate energy nuclear reactions where pion production, absorption, and emission are important channels. We study a large variety of characteristics of different types of nuclear reactions from a unique point of view, without fitting any parameters except for several versions of pion transparencies. Two results of this study, one “good” and one “bad”, are shown in Fig. 8. The general conclusion we drawn from our analysis is that imposing some transparency for pions in CEM95 improves description of parts of the NCX, SCX, and DCX pion spectra around the $\Delta(1232)$ resonance region (see the upper plot in Fig. 8) as well as of the 100–200 MeV region of backward nucleon spectra from nucleon- and pion-induced reactions. At the same time, incorporation of such pion transparency destroys the self-consistency of the CEM95 and results in a clear overestimation of pion production at forward angles (see the lower plot in Fig. 8) for different reactions. We interpret these results as an indication that we need a further improvement of the treatment of pion-nucleus interactions in CEM95 (e.g., inclusion of Δ and other resonances explicitly as cascade participants, a better approximation of experimental πN and NN angular distributions and of pion absorption in the CEM) rather than as evidence of new physics related with some exotic pion transparency.

E. Pion Absorption. The pion absorption cross section on nuclear pairs is treated in CEM95 according to Eq. (4), using experimental data for absorption on deuterons. Calculations by many authors reveal that an overall satisfactory description of different experimental data can be obtained over a large range of pion energies and target nuclei, provided that the “effective” approximation $W \simeq \text{const} = 4$ is used. The probability of absorption of pions on different pp , np , and nn pairs is taken to be the same, whenever the absorption is allowed by the charge conservation law. This is quite a rough approximation and we have encountered problems using it to study pion-nucleus interactions in the Δ resonance region [3].

If we assume that pions are absorbed on nucleon pairs only through the production with subsequent absorption of Δ isobars, $\pi[NN] \rightarrow \Delta N \rightarrow NN$, than from the isospin decomposition one gets the

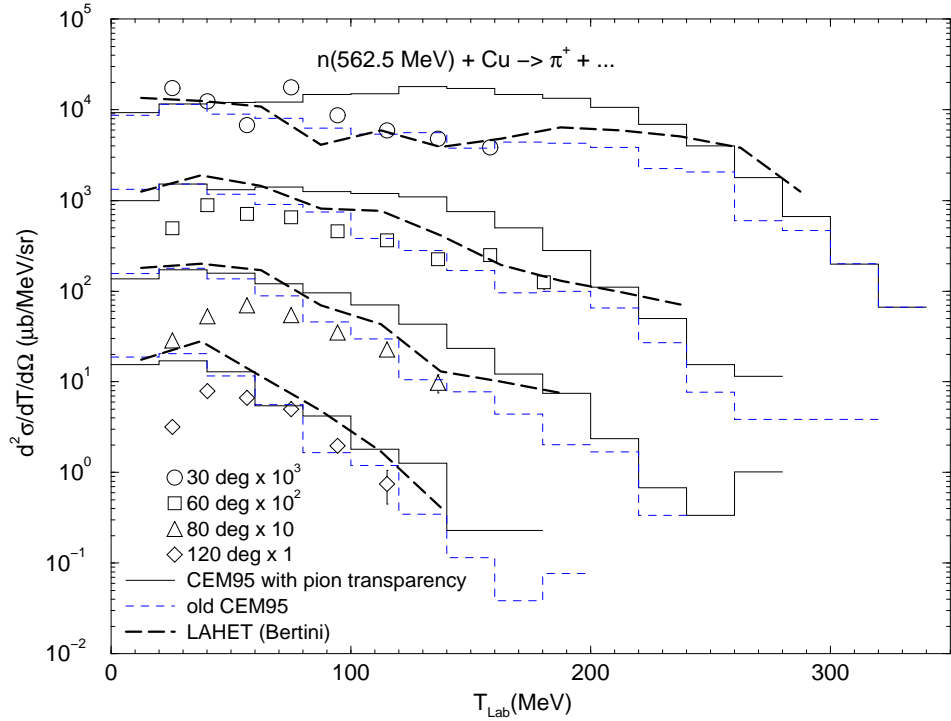
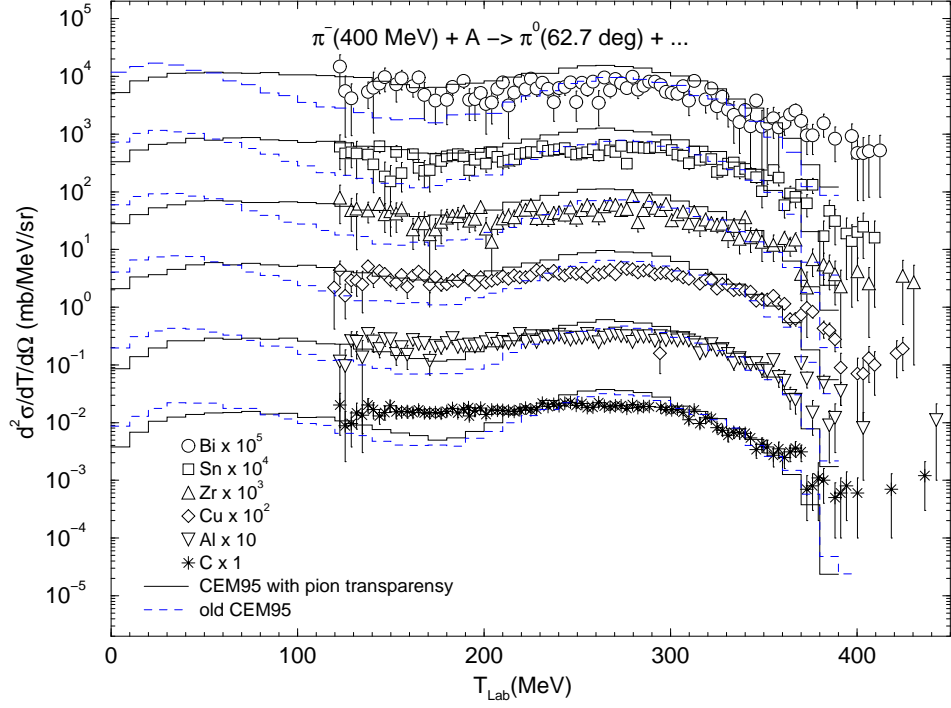


Fig. 8. Comparison of experimental SCX [45] π^0 spectra from 400 MeV π^- on different targets [52] and of π^+ spectra from 562.5 MeV neutrons on Cu [56] with results of CEM95 calculations with pion transparency, i.e., with an imposed $\lambda_\pi \geq 2$ fm for pions from $(\pi, 2\pi)$ interactions and $\lambda_\pi \geq 1.2$ fm for all pions after the first πN interaction (solid histograms) and with standard CEM95 results (dashed histograms). For comparison, the thick dashed lines show results of LAHET (Bertini INC) [33] calculations from [56].

following absorption ratios [57]:

$$\begin{aligned}
\frac{\sigma_{\pi^+}(nn) \rightarrow np}{\sigma_{\pi^+}(np) \rightarrow pp} &= 0.083, & \frac{\sigma_{\pi^0}(np) \rightarrow np}{\sigma_{\pi^+}(np) \rightarrow pp} &= 0.440, & \frac{\sigma_{\pi^0}(nn) \rightarrow nn}{\sigma_{\pi^+}(np) \rightarrow pp} &= 0.140, \\
\frac{\sigma_{\pi^0}(pp) \rightarrow pp}{\sigma_{\pi^+}(np) \rightarrow pp} &= 0.140, & \frac{\sigma_{\pi^-}(pp) \rightarrow np}{\sigma_{\pi^+}(np) \rightarrow pp} &= 0.083, & \frac{\sigma_{\pi^-}(np) \rightarrow nn}{\sigma_{\pi^+}(np) \rightarrow pp} &= 1.
\end{aligned} \tag{5}$$

To test this approximation, we started with the compilation of all presently available experimental cross sections for pion absorption on deuterons. Then, we estimate $\sigma_{\pi^-}(np) \rightarrow nn$ using Eq. (4) with $W = 4$. All other absorption cross sections, for other types of nucleon pairs and/or charges of pions are calculated according to Eq. (5). With such modifications, we study several characteristics of nuclear reactions determined mainly by pion absorption on nucleon pairs.

Pion absorption makes a large contribution to spectra of secondary nucleons emitted at very backward angles in the energy region around 140 MeV (see, e.g., [2]). Our first results, for backward proton spectra from proton-induced reactions, are very encouraging (see the upper plot in Fig. 9); using the ratios (5) for pion absorption significantly improves the agreement of calculated spectra with the data. But when we try these ratios for neutron spectra we get, as in the case of pion transparency, an opposite result; neutron yields from the pion absorption mode is strongly overestimated when using the ratios (5). We note that a variation of the absolute normalization of the pion absorption cross section, i.e., of W would not solve this problem, since if we use a smaller value for W to adjust the neutron yields, then the proton yields from pion absorption will be too low. This negative result leads us to reject the ratios (5) for CEM and to return to equal probabilities of pion absorption on different nuclear pairs.

In Fig. 9, both proton and neutron spectra at backward angles calculated with CEM95 (i.e., using equal probabilities for pion absorption on different pairs) lie above the data by a factor of 2 at energies around 100 MeV. These nucleons come in our model mainly from pion absorption. This means that pion absorption cross sections used for these targets were too high and W in Eq. (4) should be smaller. Similar results were obtained with CEM95 for other light and medium targets. To improve this situation, we re-examined the value of W . Fortunately, we presently have reliable spectra of both protons and neutrons measured at backward angles for the same targets by the same experimentalists at energies around 100–200 MeV [62]. In Fig. 10, we show part of our results: experimental spectra [62] of neutrons and protons emitted at 140° from the interaction of 1 GeV protons with different nuclei are compared with standard CEM95 calculations and using twice lower pion absorption cross sections, i.e., $W = 2$ for all targets. One can see that for medium and light nuclei, the results obtained using $W = 2$ agree much better with data as compared with the standard CEM95 results ($W = 4$). From these and similar results obtained for other targets at other intermediate energies we can conclude that W seems to depend on the atomic number of the target; increasing from about 2 for light targets like C to about 4 for heavy targets like Pb. Fig. 11, where we show results obtained with $W = 2$ for C, $W = 3$ for Fe and Ni, and $W = 4$ for Pb, serves as a confirmation of this conclusion: Introduction of a pion absorption cross section increasing with A on nuclear pairs significantly improves the agreement with data both for neutron and proton spectra at backward angles around 100–200 MeV. Similar results were obtained for other reactions. We have not yet fixed the value of W in our new version of the code, as we wish to perform several more test calculations to determine W more accurately. But we already see that we will need to use an A -dependent function for W , which increases from about 2 for C to about 4 for Pb.

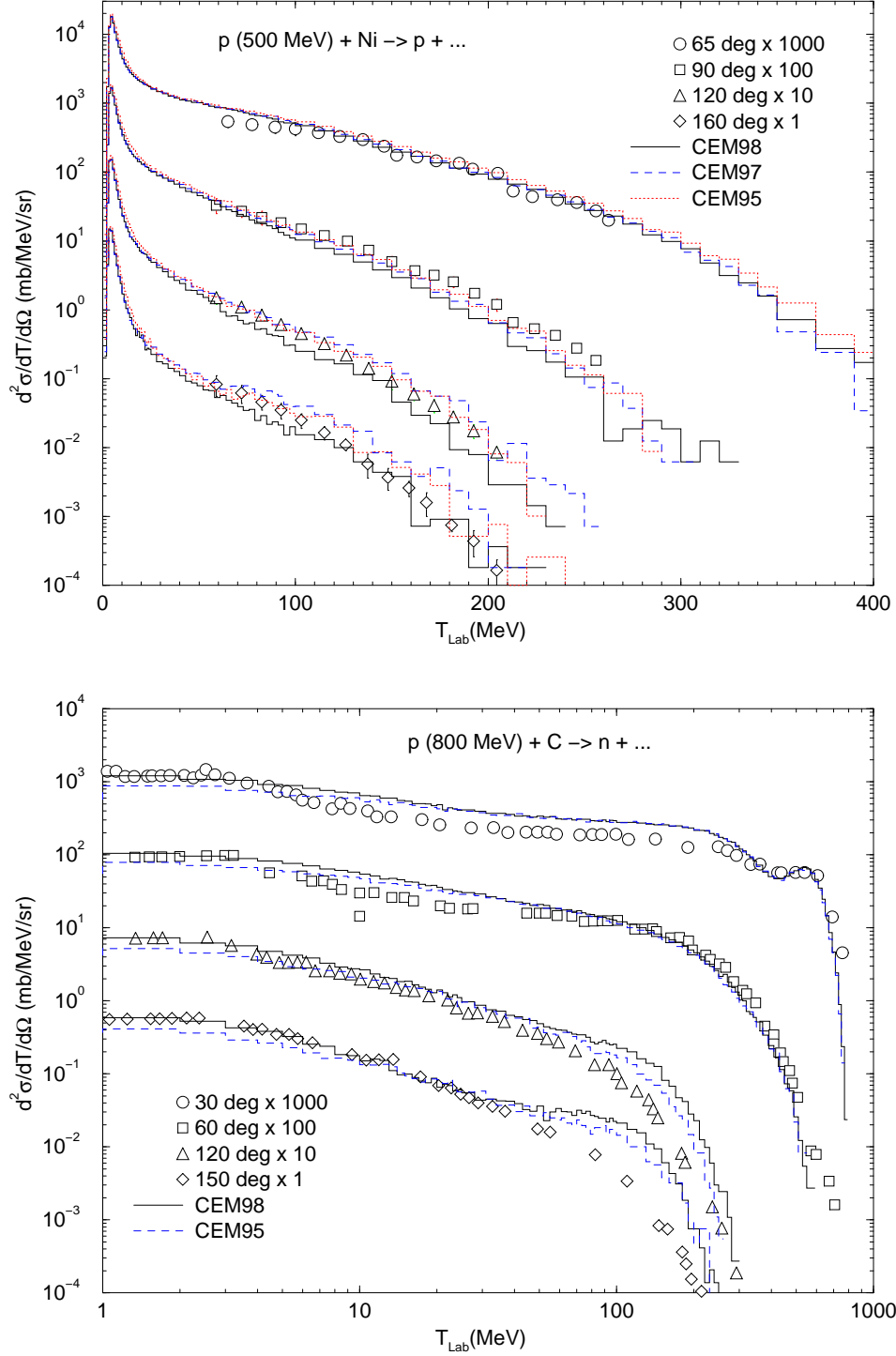


Fig. 9. Experimental proton spectra from 500 MeV p + Ni [60] and neutron spectra from 800 MeV p + C [61] compared with standard CEM95 results and with modified calculations of pion absorption cross sections according to [57] (noted in this figure as CEM98) as described in the text. CEM97 results are obtained with the same pion absorption cross sections as the CEM95 ones, but with new elementary NN and πN cross sections and new nuclear masses.

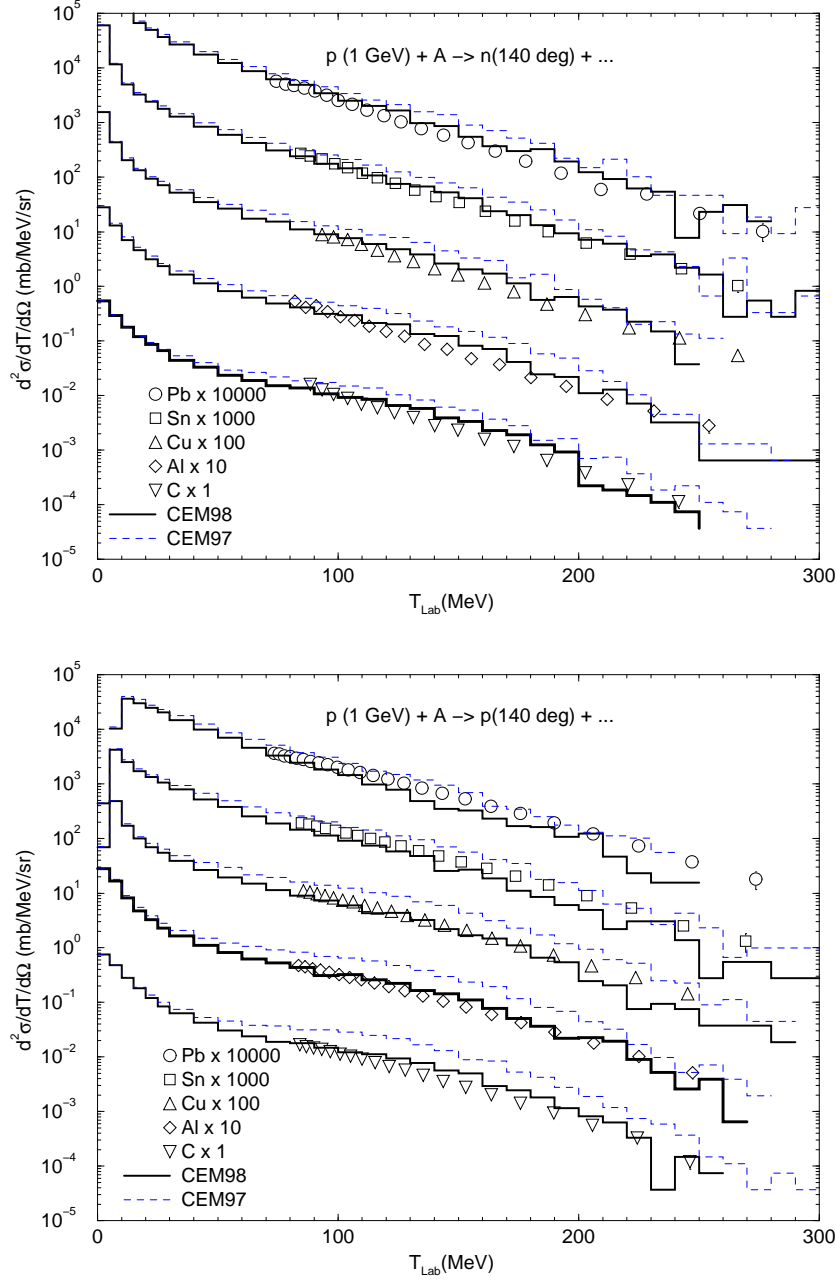


Fig. 10. Experimental spectra of neutrons and protons emitted at 140 degrees from interactions of 1.0 GeV protons with C, Al, Cu, Sn, and Pb [62] compared with standard CEM97 results (dashed histograms) and with calculations using one-half the pion absorbtion cross sections, i.e., $W = 2$, or: $\sigma_{abs}(\pi + [NN]) = 2\sigma_{abs}(\pi + d)$ (noted here as CEM98).

F. Other Enhancements, CEM97a Code, and Further Work. We have made a number of other improvements to CEM95 concerning the description of the preequilibrium and evaporation stages of reactions. This includes incorporating a complete experimental mass table extended by the Moller-Nix mass calculations [58], along with corresponding ground-state microscopic corrections and pairing energies. We have also implemented a new level-density approximation which incorporates the calculated microscopic corrections and pairing energies and angular momentum dependent macroscopic fission barriers [59],

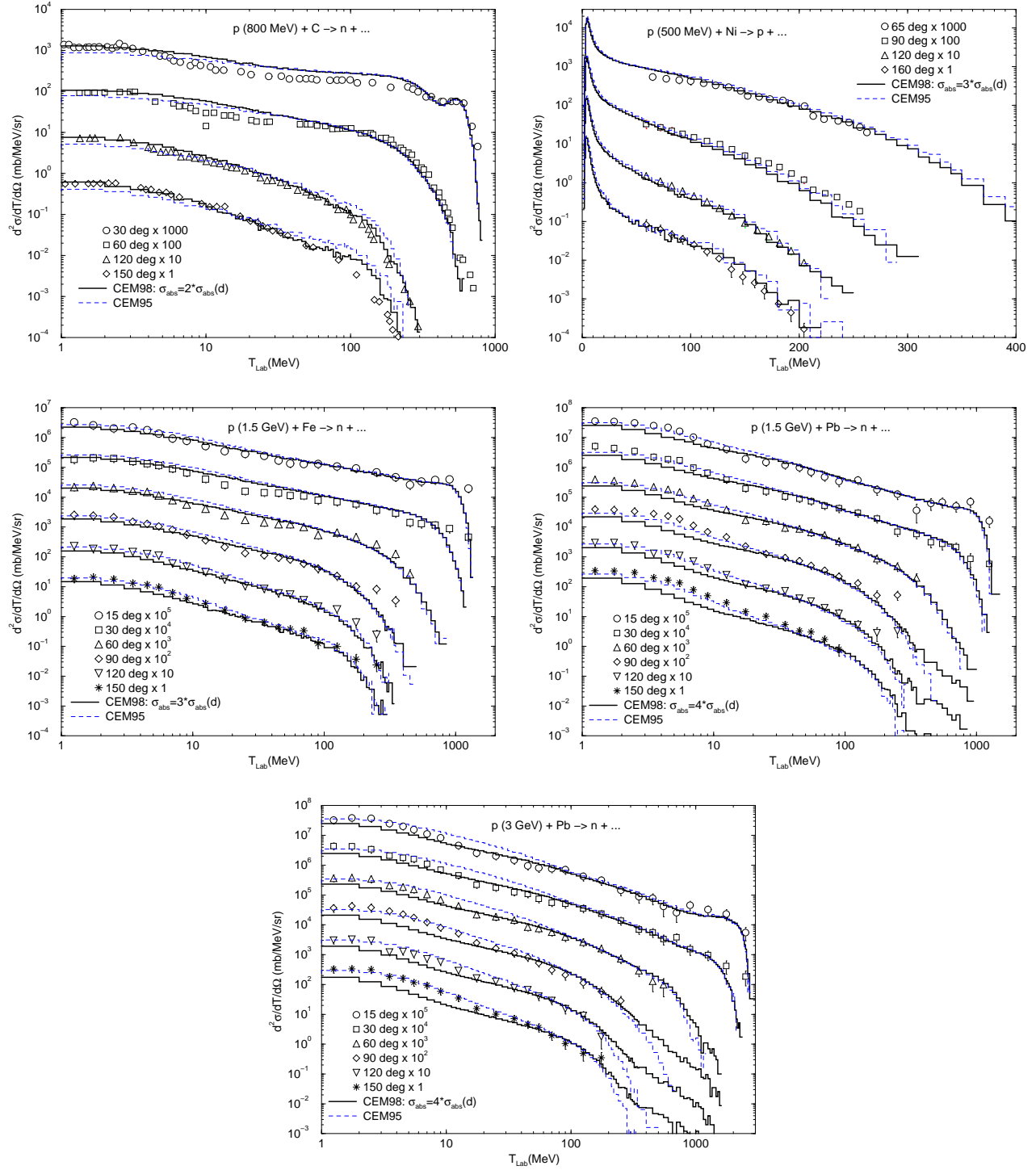


Fig. 11. Comparison of experimental neutron (proton, for 500 MeV protons on Ni) spectra from interactions of protons of 800 MeV on C [61], 500 MeV on Ni [60], 1.5 GeV on Fe and Pb [29], and 3.0 GeV on Pb [29], with standard CEM95 results (dashed histograms) and with calculations using modified pion absorption cross sections on quasideuterons, namely, $W = 2$ for the light C target, $W = 3$ for the medium mass Ni and Fe targets, and $W = 4$ for the heavy Pb target (noted here as CEM98).

which are consistent with the macroscopic model used in the Moller-Nix mass calculations. We have significantly improved the treatment of rotational energy and have made a number of small refinements to the code like using actual updated values for the masses of elementary particles (for simplicity in CEM95, we used, e.g., $m_\pi = 140$ MeV for pions of any charges and $m_n = m_p = 940$ MeV) and more precise values for physical constants.

With these modifications and various coding improvements, we wrote a preliminary improved version of the CEM95 code called CEM97a, which is now incorporated in the MCNPX transport code [17].

CEM97a is a preliminary release, since several improvements have been made after its creation and we continue the work in this direction, but already CEM97a provides a much better description of many data than the initial code, CEM95. As an example, in Fig. 12 we show excitation functions for production of all Xe isotopes for which we found experimental data from $p+^{133}\text{Cs}$ interactions, part of our calculations for a medical isotope production study [9], using the standard CEM95 and with the improved version CEM97a. All available experimental data and calculations with the LAHET [33] code system (version 2.83) by K. A. Van Riper from [9] and with the HMS-ALICE code [39] by M. B. Chadwick from the LA150 Activation Library [64] are shown as well, for comparison. One can see that CEM97a describes these data much better than CEM95 and LAHET, and the difference between predictions of the new and old versions of CEM increases as the isotopes produced become more neutron deficient, reaching a factor of 3 for ^{120}Xe . Such a big difference between results from the new and old versions of the code is related mainly to using experimental nuclear masses and binding energies in CEM97a and the 40 year old approximations of Cameron [66] in CEM95.

An example of the importance of using reliable values for nuclear masses can be seen also in Fig. 11. From this figure one can see that neutron spectra from Pb calculated with CEM95 agree very well with the data at low energies, in the evaporation parts of spectra. This is not necessarily good, since the calculations with CEM95 for Pb take into account competition between evaporation and fission, but the fission itself is not calculated; when a fission event occurs after the cascade and preequilibrium stages of a reaction, CEM95 stores this event to calculate a fission cross section, but then it stops further simulation of this event. That is, calculated spectra do not contain contributions of particles evaporated from fragments following fission. We are presently working to incorporate simulation of the fission processes themselves into the CEM, and we need some “room” for particles evaporated from fission fragments. As we see from Fig. 11, the new version (noted as CEM98) of the code provides us such “room”; calculated spectra agree very well with the data for intermediate and high energy parts of the spectra but lie below the measurements in the evaporation region by a factor of 2, leaving some place for neutrons evaporated from fission fragments.

After creating CEM97a, we have further improved the code. We have improved the approximation to the level densities at the fission saddle point and have introduced other modifications, given separately in [65]. We also further modified the cascade modeling in the code by improving the treatment of photo-nuclear reactions and imposing energy and momentum conservation for the whole cascade stage of a reaction using experimental nuclear masses and binding energies for incident and emitted nucleons instead of the old approximations of CEM95.

Our improvement efforts continue. We have written a subroutine for emission of complex particles at the cascade stage of reactions via the mechanism of their coalescence from emitted nucleons, have modified the preequilibrium and evaporation stages to allow emission of fragments with $A > 4$ from not too light excited nuclei, and are working now to develop an appropriate model for high energy fission. Among many other things, we need to improve the approximation of the inverse cross sections used in calculating particle emission widths and to treat more accurately α -emission at both the preequilibrium and evaporation stages.

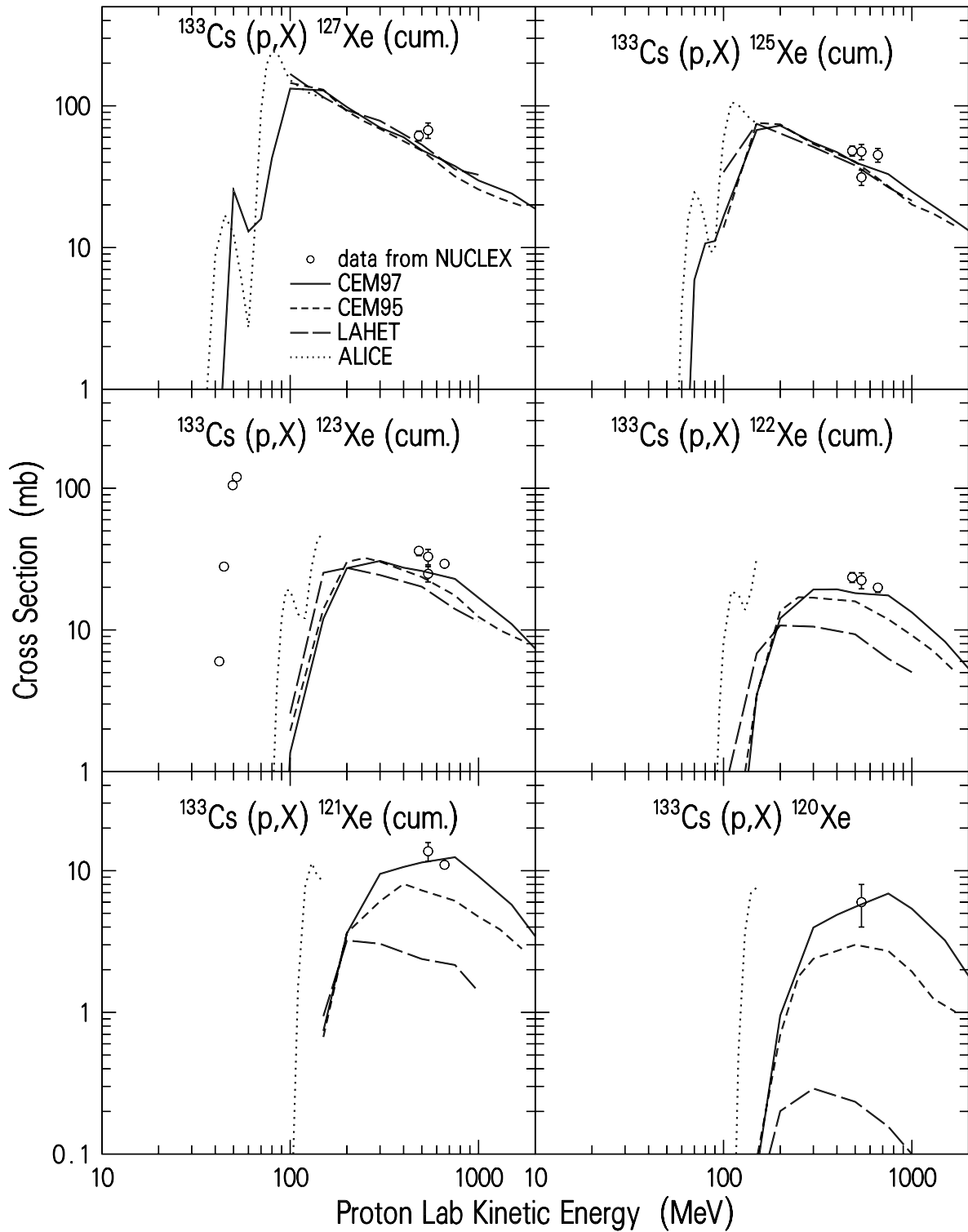


Fig. 12. Excitation functions for the production of $^{127-120}\text{Xe}$ from $p+^{133}\text{Cs}$. Calculations with the new CEM97a code are shown by solid lines and with the standard CEM95 by short dashed lines. Results of calculations with the LAHET [33] code system (version 2.83) by K. A. Van Riper from Ref. [9] are shown by long dashed lines and results of the HMS-ALICE code [39] calculated by M. B. Chadwick from the LA150 Activation Library [64] are shown by dotted lines. Experimental data are from the compilation [63].

4. Summary

In this paper, we have demonstrated the good overall predictive power of the modified version of the CEM as realized in the code CEM95. Then, to improve the agreement of its results with experimental data and to make it a better tool for applications, we modify it further, progressively incorporating features of previously neglected physics. So far, we have incorporated in the CEM new and better approximations for the elementary cross sections, imposed momentum-energy conservation for each simulated event, used more precise values for nuclear masses, Q -values, binding and pairing energies, corrected systematics for the level density parameters, studied and chosen the optimal approximations for the pion “binding energy”, V_π , for the cross sections of pion absorption on quasideuteron pairs inside a nucleus, for the effects of refractions and reflections, and for nuclear transparency of pions. We also make a number of refinements in calculation of the fission channel, described separately in [65].

As it was shown by a number of examples, the improvements to the CEM made so far clearly have increased its predictive power. Our work is not finished. Among improvements of the CEM which are of highest priority we consider development and incorporation of an appropriate model of high-energy fission, treating more accurately α -emission at both preequilibrium and evaporative stages, incorporation of a model of fragmentation of medium and heavy nuclei, possibly the Fermi breakup model for highly excited light nuclei, modeling evaporation and preequilibrium emission of fragments with $A > 4$, and improvement of the approximation for inverse cross sections.

The problems discussed above are typical not only for the CEM, but also for all other similar models and codes, where they are also not yet solved.

Acknowledgements

We express our gratitude to K. Ishibashi, S. Chiba, J. D. Zumbro, R. J. Peterson, V. V. Vikhrov, and B. Bassaleck for suppling us with numerical values of their measurements and we thank K. Ukai for kindly providing us with his and T. Nakamura’s 1997 compilation “*Data Compilation of Single Pion Photoproduction Below 2 GeV*” used in our work. We are grateful to R. E. MacFarlane and L. S. Waters for helpful discussions and support of the present work. We thank many users of the CEM codes, especially V. F. Batyaev, O. Bersillon, F. Gallmeier, N. V. Mokhov, and A. V. Prokofiev, for their constructive contributions, which led to the removal of several bugs and to improvements in the model. This study was supported by the U. S. Department of Energy.

References

- [1] K. K. Gudima, S. G. Mashnik, and V. D. Toneev, *Nucl. Phys.* **A401**, (1983) 329.
- [2] S. G. Mashnik, *Nucl. Phys.* **A568**, (1994) 703 and references therein.
- [3] S. G. Mashnik, *Yad. Fiz.* **58**, (1995) 1772 [*Phys. At. Nucl.* **58**, (1995) 1672]; *Acta Phys. Pol.* **B24**, (1993) 1685; *Rev. Roum. Phys.* **37**, (1992) 179.
- [4] T. Gabriel, G. Maino, and S. G. Mashnik, *Proc. XII International Seminar on High Energy Problems “Relativistic Nucl. Phys. & Quantum Chromodynamics”, Dubna, Russia, 12–17 September, 1994*, JINR E1, 2-97-79 (1997) p. 309; C. Y. Fu, T. A. Gabriel, and R. A. Lillie, *Proc. 3rd Specialists Meeting on Shielding Aspects of Accelerators, Targets and Irradiation Facilities (SATIF-3), Tohoku University, Sendai, Japan, May 12–13, 1997*, NEA/OECD (1998) p. 49.
- [5] S. G. Mashnik, *Acta Phys. Slovaca* **43**, (1993) 86; *ibid.*, p. 243.

- [6] S. G. Mashnik, *Izv. Rossiiskoi Akad. Nauk, Ser. Fiz.* **60**, (1996) 73 [*Bull. Russian Acad. Sci.: Physics* **60**, (1996) 58].
- [7] S. G. Mashnik, A. J. Sierk, O. Bersillon, and T. A. Gabriel, *Nucl. Instr. Meth.* **A414**, (1998) 68; LANL Report LA-UR-97-2905 (1997); <http://t2.lanl.gov/publications/publications.html>.
- [8] Yu. E. Titarenko et al., *Nucl. Instr. Meth.* **A414**, (1998) 73 and references therein.
- [9] K. A. Van Riper, S. G. Mashnik, M. B. Chadwick, M. Herman, A. J. Koning, E. J. Pitcher, A. J. Sierk, G. J. Van Tuyle, L. S. Waters, and W. B. Wilson, LANL Report LA-UR-97-5068 (1997); <http://t2.lanl.gov/publications/publications.html>; K. A. Van Riper, S. G. Mashnik, and W. B. Wilson, "Study of Isotope Production in High Power Accelerators," LA-UR-98-5378, this conference.
- [10] R. Michel and P. Nagel, *International Codes and Model Intercomparison for Intermediate Energy Activation Yields*, NSC/DOC(97)-1, OECD, Paris (1997); <http://www.nea.fr/html/science/pt/ieay>.
- [11] V. A. Konshin, *JAERI-Research 95-036*, JAERI (1995).
- [12] A. V. Prokofiev, S. G. Mashnik, and A. J. Sierk, *Proc. Int. Conf. on the Phys. of Nucl. Sci. and Technology, Islandia Marriott Long Island, Hauppauge, New York, October 5–8, 1998*, ANS, La Grange Park, Illinois 60526 USA (1998), Vol. 1, p. 678; LANL Report LA-UR-98-0418, Los Alamos (1998); E-print **nucl-th/9802027**; to be published in *Nucl. Sci. Eng.*, January 1999.
- [13] N. V. Mokhov, S. I. Striganov, A. Van Ginneken, S. G. Mashnik, A. J. Sierk, and J. Ranft, "MARS Code Developments," Fermilab-Conf-98/379 (1998), LA-UR-5716 (1998), this conference.
- [14] Yu. E. Titarenko, O. V. Shvedov, V. F. Batyaev, E. I. Karpikhin, M. M. Igumnov, V. I. Volk, A. Yu. Vakhrushin, S. V. Shepelkov, A. V. Lopatkin, A. N. Sosnin, S. G. Mashnik, R. E. Prael, M. B. Chadwick, and T. A. Gabriel, "Experimental Measurement and Computer Simulation Study of Radionuclide Formation in the ADT Materials Irradiated with Intermediate Energy Protons," *Proc. Second Int. Topical Meeting on Nuclear Applications of Accelerator Technology (AccApp'98), Gatlinburg, TN, USA, September 20–23, 1998*.
- [15] K. C. Chandler and T. W. Armstrong, *Nucl. Sci. Eng.* **49**, (1972) 110.
- [16] O. Bersillon et al., *Proc. Int. Conf. on Nucl. Data for Science and Technology, Trieste, Italy, May 19–24, 1997*, p. 257; see the Web page at: http://www-phys.llnl.gov/N_Div/APT/trispal.html.
- [17] F. Gallmeier, "Implementation of the CEM Code into MCNPX," this conference.
- [18] R. Buck and E. Lent, "COG: A New, High-Resolution Code for Modeling Radiation Transport," *Energy & Technology Review*, University of California, Lawrence Livermore National Laboratory, **June 1993**, p. 9 and to be published.
- [19] K. K. Gudima, G. A. Ososkov, and V. D. Toneev, *Sov. J. Nucl. Phys.* **21**, (1975) 138; S. G. Mashnik and V. D. Toneev, *JINR Communication P4-8417*, Dubna (1974).
- [20] S. G. Mashnik, *User Manual for the Code CEM95*, OECD NEA Data Bank, Paris, France (1995); <http://www.nea.fr/abs/html/iaea1247.html>.
- [21] C. Y. Fu and T. A. Gabriel, *Proc. 3rd Workshop on Simulating Accelerator Radiation Environments (SARE3), KEK, Tsukuba, Japan, May 7–9, 1997*, p. 315.
- [22] A. V. Dementyev and N. M. Sobolevsky, *Proc. 3rd Workshop on Simulating Accelerator Radiation Environments (SARE3), KEK, Tsukuba, Japan, May 7–9, 1997*, H. Hirayama, Ed., KEK Proceedings 97-5, June 1997, H/R/D, p. 21.

- [23] N. Yoshizawa, K. Ishibashi, and H. Takada, *J. Nucl. Sci. Technol.* **32**, (1995) 601.
- [24] N. Shigyo, K. Ishibashi, N. Yoshizawa, and H. Takada, *Proc. Int. Conf. on Nucl. Data for Science and Technology, Trieste, Italy, May 19–24, 1997*,
- [25] V. S. Barashenkov et al., “CASCADE” Program Complex for Monte Carlo Simulation of Nuclear Processes Initiated by High Energy Particles and Nuclei in Gaseous and Condensed Matter,” (in Russian) Preprint JINR P2-85-173, Dubna, USSR, 1985.
- [26] N. V. Stepanov, Institute for Theoretical and Experimental Physics (Moscow, Russia) Preprints: *ITEP-55-88 (1988)*, *ITEP-81 (1987)*, *ITEP-129 (1985)*, *ITEP-91 (1991)*; N. V. Stepanov, Ph.D. Thesis, Moscow State Univ. (1990).
- [27] M. Blann, H. Gruppelaar, P. Nagel, and J. Rodens, *International Code Comparison for Intermediate Energy Nuclear Data*, NEA OECD, Paris (1994).
- [28] S. G. Mashnik, *Proc. Specialists’ Mtg. “Intermediate Energy Nuclear Data: Models and Codes,” Issy-les-Moulineaux, France, May 30–June 1, 1994*, OECD, Paris (1994), p. 107.
- [29] K. Ishibashi et al., *J. Nucl. Sci. Techn.* **34**, (1997) 529.
- [30] M. M. Meier et al., *Nucl. Sci. Eng.* **110**, (1992) 289; tabulated data available in the data base EXFOR.
- [31] S. Stamer et al., *Phys. Rev. C* **47**, (1993) 1647; tabulated data available in the data base EXFOR.
- [32] T. Nakamoto et al., *J. Nucl. Sci. and Techn.* **34**, (1997) 860.
- [33] R. E. Prael and H. Lichtenstein, “User Guide to LCS: The LAHET Code System,” *LA-UR-89-3014*, LANL (September 1989).
- [34] J. Cugnon, C. Volant, and S. Vuillier, *Nucl. Phys.* **A620**, (1997) 475.
- [35] S. Cierjacks et al., *Phys. Rev. C* **36**, (1987) 1976; P. Cloth et al., KFA Jülich Report Jüe-2208, 1988.
- [36] N. Shigyo, K. Iga, and K. Ishibashi, *JAERI-Conf 97-005*, 291 (1997).
- [37] R. Michel and P. Nagel, *International Codes and Model Intercomparison for Intermediate Energy Activation Yields*, NEA/OECD, Paris, 1997, NSC/DOC(97)-1.
- [38] Yu. E. Titarenko and co-authors from ITEP, H. Yasuda, H. Takada, Y. Kasugai, S. Chiba, R. E. Prael, M. B. Chadwick, S. G. Mashnik, T. A. Gabriel, M. Blann, and R. Michel, Interim Technical Report on the Feasibility Study Stage of the ISTC Project # 839 Entitled *Experimental and Theoretical Study of the Yields of Residual Product Nuclei Produced in Thin Targets Irradiated by 100–2600 MeV Protons*, ISTC 839-97, Moscow, April 1998.
- [39] M. Blann, *Phys. Rev. C* **54**, (1996) 1341; M. Blann and M. B. Chadwick, *Phys. Rev. C* **57**, (1998) 233.
- [40] R. Silberberg and C. H. Tsao, *Astrophys. J.* **220**, (1973) 315; 335 and private communication from C. H. Tsao.
- [41] “*Proc. Second Intl. Conf. on Accelerator-Driven Transmutation Technologies and Applications*,” Kalmar, Sweden, June 3–7, 1996, Vols. 1 and 2, H. Condé, Ed., Uppsala University (1997).
- [42] V. S. Barashenkov and V. D. Toneev, *Interaction of High Energy Particles and Nuclei with Atomic Nuclei*, (in Russian) Atomizdat, Moscow (1972).
- [43] S. G. Mashnik and A. J. Sierk, *Nucleon-, Pion-, and Gamma-Nucleon Cross Sections*, to be published.

- [44] A. S. Iljinov, *Code for Calculations of Intranuclear Cascades at Energies $T \leq 5$ GeV*, JINR Report B1-4-5478, Dubna, 1970.
- [45] S. Hoibraten, Ph.D. thesis U. of Colorado, Los Alamos, LA-11582-T, UC-414, May, 1989.
- [46] V. S. Barashenkov, *Pion-Nucleus Cross Sections*, JINR Communication P2-90-158, Dubna, 1990.
- [47] K. Chen et al., *Phys. Rev.*, **166** (1968) 948.
- [48] V. S. Barashenkov, K. K. Gudima, and V. D. Toneev, *Acta Phys. Pol.* **36**, (1969) 457.
- [49] A. S. Iljinov, V. I. Nazaruk, and S. E. Chigrinov, *Yad. Fiz.* **36**, (1982) 646 [*Sov. J. Nucl. Phys.* **36**, (1982) 376]; *Nucl. Phys.* **A382**, (1982) 378.
- [50] A. S. Iljinov et al., *Nucl. Phys.* **A616**, (1997) 575.
- [51] J. D. Zumbro et al., *Phys. Rev. Lett.* **71**, (1993) 1796.
- [52] J. Ouyang, Ph.D. thesis U. of Colorado, Los Alamos, LA-12457-T, UC-413, Dec., 1992.
- [53] S. A. Wood et al., *Phys. Rev. C* **46**, (1992) 1903.
- [54] W. R. Gibbs and W. B. Kaufmann, in *Pion-Nucleus Physics: Future Directions and New Facilities at LAMPF, Los Alamos, New Mexico, 1987*, edited by R. J. Peterson and D. D. Strottman, AIP Conference Proceeding No. 163 (AIP, New York, 1988), p. 279; D. Strotmann and W. R. Gibbs, *Phys. Lett.* **B149**, (1984) 288; W. R. Gibbs and J. W. Kruk, *Z. Phys.* **C46**, (1990) S45;
- [55] A. K. Michael, R. J. Peterson, S. G. Mashnik, and A. J. Sierk, *University of Colorado Nuclear Physics Laboratory Annual Report*, Boulder, 1997.
- [56] M. L. Brooks et al., *Phys. Rev. C* **45**, (1992) 2343; M. L. Brooks, Ph.D. thesis, U. of New Mexico, Los Alamos, LA-12210-T, UC-910, Oct., 1991.
- [57] A. Engel et al., *Nucl. Phys.* **A572**, (1994) 657.
- [58] P. Möller, et al. *Atomic Data and Nuclear Data Tables* **59**, (1995) 185.
- [59] A. J. Sierk, *Phys. Rev. C* **33**, (1986) 2039.
- [60] G. Roy et al., *Phys. Rev. C* **23**, (1981) 1671.
- [61] W. B. Amian et al., *Nucl. Sci. Eng.* **112**, (1992) 78; tabulated data available in the data base EXFOR.
- [62] V. N. Baturin, V. V. Vikhrov, E. N. Komarov, M. M. Makarov, S. G. Mashnik, V. V. Nelyubin, and V. V. Sulimov, *Measurement of the Neutron and Proton Spectra at 94° and 120° Produced by 1 GeV Protons on C and Pb*, Leningrad Institute of Nuclear Physics Preprint No. 1302, Leningrad, Russia (1987) and private communication from V. V. Vikhrov (1998).
- [63] A. S. Iljinov et al., Springer Verlag, Landolt-Börnstein, New Series, subvolumes **I/13a** (1991), **I/13b** (1992), **I/13c** (1993), and **I/13d** (1994); V. I. Ivanov, N. M. Sobolevsky, and V. G. Semenov, *Proc. 3rd Specialists Meeting on Shielding Aspects of Accelerators, Targets and Irradiation Facilities (SATIF-3)*, Tohoku University, Sendai, Japan, May 12–13, 1997, NEA/OECD (1998) p. 277.
- [64] M. B. Chadwick, private communication on 150 MeV n & p calculations, to be published.
- [65] A. J. Sierk and S. G. Mashnik, “Modeling Fission in the Cascade-Exciton Model,” this conference.
- [66] A. G. W. Cameron, *Can. J. Phys.* **35**, (1957) 1021.